

ADVANCES IN PARALLEL FINITE ELEMENT CODE SUITE ACE3P*

Lixin Ge, Kwok Ko, Oleksiy Kononenko, Zenghai Li, Cho-Kuen Ng¹, Liling Xiao,
SLAC, Menlo Park, CA 94025, USA
Ji Qiang, LBNL, Berkeley, CA 94720, USA

Abstract

New capabilities in SLAC's parallel finite element electromagnetics simulation suite ACE3P are reported. These include integrated electromagnetic (Omega3P), thermal and mechanical (TEM3P) modules for multi-physics modeling, an interface to particle-material interaction codes for calculation of radiation effects due to dark current generation (Track3P), and coupled electromagnetic (ACE3P) and beam dynamics (IMPACT) simulation. Results from these applications are presented.

INTRODUCTION

SLAC has developed the electromagnetics simulation suite **ACE3P** (Advanced Computational Electromagnetics 3D Parallel), consisting of modules in frequency and time domains [1]. These massively parallel codes are based on the high-order finite-element method so that geometries of complex structures can be represented with high fidelity through conformal grids, and high solution accuracies can be obtained using high-order basis functions in finite elements. **ACE3P** consists of the following modules: **Omega3P**, an eigensolver for cavity mode (damping) calculations; **S3P**, a frequency-domain solver to calculate S-parameters of rf components; **T3P**, a time-domain solver for transients and wakefield computations; **Track3P**, a particle tracking code for multipacting and dark current studies; **Pic3P**, a particle-in-cell code for self-consistent particle and field interactions; **TEM3P**, a multi-physics code for integrated electromagnetic, thermal and mechanical effects. Running on DOE supercomputing facilities, these six applications modules have been applied to a wide range of modeling and simulation problems for accelerators [2].

Recent advances in the modeling capabilities of **ACE3P** have been focused on enhancing the multi-physics module **TEM3P** and the integration of **ACE3P** modules with other application codes. The major improvements include

- Benchmarking **TEM3P** thermal calculations for a realistic 3D structure against measurement;
- Development of a mechanical eigensolver in **TEM3P** to determine mechanical modes of a superconducting (SRF) cavity to facilitate the investigation of microphonics [3];
- Development of an electro-mechanical analysis tool to decompose the Lorentz force displacement into those of the mechanical modes of an SRF cavity;
- Integration of **ACE3P** with the beam dynamics code **IMPACT** for realistic calculation of beam emittance

in accelerator structures and systems;

- Interface of **ACE3P** to particle-material interaction codes such as Geant4 and Fluka for evaluating radiation effects in accelerators.

In the following sections, simulation results from these applications are presented.

THERMAL CALCULATIONS FOR LCLS-II COUPLER

The LCLS-II adopts the TTF3 coaxial fundamental power coupler with modest modifications to make it suitable for CW operation. The coupler consists of a cold section and a warm section made of different kinds of materials with a thin copper coating at the warm side. The fully 3D geometry of the coupler is modeled using **TEM3P** to determine the temperature distribution along the feedthrough of the coupler [4]. The temperature distribution shown in Fig. 1 is obtained for using 6 kW power for the standing wave on resonance. The maximum temperature is found at the bellows located near the central region of the coupler, and it agrees well with the value from high power tests at Fermilab, as shown in Fig. 2 [5].

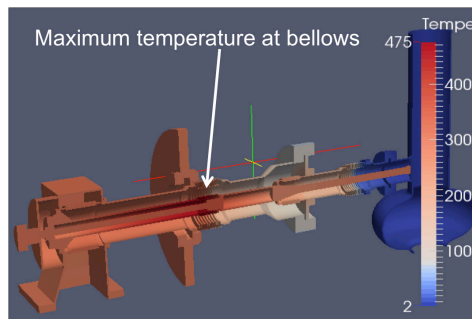


Figure 1: Temperature distribution in TTF3 coupler calculated using TEM3P.

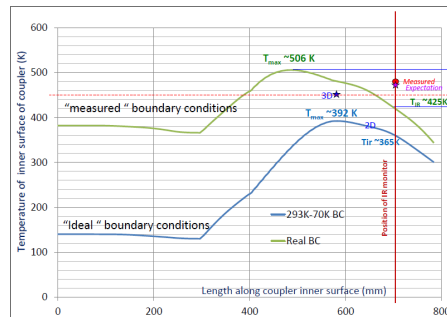


Figure 2: Temperature along the inner conductor with the red dot showing the agreement of simulation and measurement.

* This work was supported by DOE Contract No. DE-AC02-76SF00515.

¹cho@slac.stanford.edu

The simulation has been made feasible by the availability of shell elements in **TEM3P**, which enables the modeling of the thin copper coating on the conductor wall without the use of extremely small elements. In addition, parallel computation through the use of multiple processors allows for high-resolution simulation by taking advantages of large memory and speedup.

MECHANICAL CALCULATIONS FOR LCLS-II SRF CAVITY

An SRF cavity is subject to mechanical deformation from the electromagnetic pressure exerted on the cavity wall by the accelerating mode of the cavity, which leads to Lorentz force detuning due to the frequency shift arising from the deformation. The determination of Lorentz force detuning requires an electro-mechanical calculation, where the electromagnetic field is first calculated using **Omega3P** for the vacuum region of the cavity and then the Lorentz force on the cavity surface will serve as the boundary condition for **TEM3P** to determine the deformation of the cavity wall. Fig. 3 shows the Lorentz force displacement of the LCLS-II SRF cavity using an accelerating gradient at 16 MV/m, with a free and a fixed boundary imposed on the left and the right end of the cavity, respectively. The displacement is largest (about 3 μm) at the free end and falls off gradually towards the fixed end.

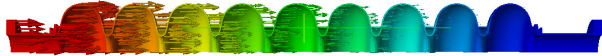


Figure 3: Lorentz force displacement of the LCLS-II SRF cavity using a quarter model of the geometry.

The study of microphonics effects due to Lorentz force detuning requires the determination of the eigenmodes for mechanical oscillations of the cavity. Using **TEM3P**'s mechanical eigensolver, the first three eigenmodes for the quarter model subject to the same boundary constraints are shown in Fig. 4. Because of the boundary conditions imposed on the symmetry planes of the quarter model, only longitudinal modes are modeled.

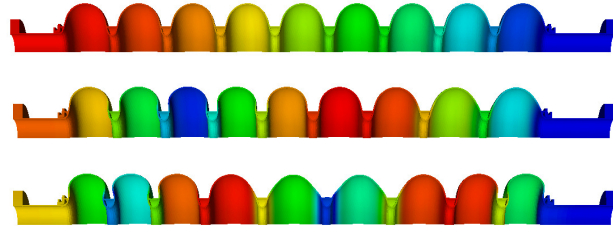


Figure 4: Mechanical modes of the LCLS-II SRF cavity with frequencies 96 Hz, 296 Hz and 496 Hz, respectively (from top to bottom).

The coupling of Lorentz force displacement to individual mechanical modes is computed by a modal decomposition. In this regard, the displacement shown in Fig. 3 is expressed as a linear combination of a complete set of displacements from the orthogonal modes:

$$\vec{u}_{LF}(x, y, z) = \sum_{i=1}^{\infty} q_i \vec{u}_i(x, y, z),$$

where q_i is the coupling coefficient of the i th mechanical mode, from which one can determine the contribution to the frequency shift by this mode if it is excited. Assuming a specified accelerating gradient E_{acc} , the Lorentz force coefficient k_i for the i th mechanical mode is calculated as

$$k_i = \Delta f_i^{RF} / E_{acc}^2.$$

Table 1 lists the decomposition of the Lorentz force displacement into the first 10 longitudinal mechanical modes of the LCLS-II SRF cavity. It can be seen that the major contributions to the total frequency shift are from the lowest several mechanical modes. The summation of the displacements by the 10 modes is very close to the value of static Lorentz force calculated by the model in Fig. 3. The frequencies and Lorentz force coefficients of the mechanical eigenmodes will provide useful information for studying microphonics effects due to Lorentz force using a feedback control algorithm [6].

Table 1: Lorentz force coefficients for the 10 lowest mechanical modes of the LCLS-II SRF cavity shown in Fig. 3.

Mode	f^{mech} [Hz]	q	Δf^{RF} [Hz]	k [Hz/MV ²]
1	99	-4.84E-06	-930	-2.21
2	297	7.51E-07	-145	-0.34
3	497	3.38E-07	-43	-0.10
4	695	2.59E-07	-36	-0.09
5	890	1.91E-07	-15	-0.04
6	1075	1.68E-07	-18	-0.04
7	1246	1.37E-07	-6	-0.01
8	1393	1.22E-07	-10	-0.02
9	1493	6.03E-08	0	0.00
10	1585	2.65E-07	-33	-0.08
Total	-	-	-1236	-2.93
Static LF	-	-	-1192	-2.83

INTEGRATION OF ACE3P AND IMPACT

IMPACT-T [7], a part of the **IMPACT** framework, is a parallel, 3D space-charge tracking code to study beam dynamics in photo-injectors and rf linear accelerators. The code can track particles using its built-in beamline element models, or using the external 3D field maps of beamline elements provided by users for more accurate modeling of 3D effects. Presently the users need to supply the field map by converting the data from a field solver. Integrating **ACE3P** with **IMPACT-T** presents a new parallel capability that combines 3D electromagnetic simulation with beam dynamics calculation so that accelerator cavities and beamline elements can be

modeled on a system scale with high accuracy. The representations of field data in terms of 3D maps and transfer maps in the two simulation software packages have been standardized to enable the transfer of cavity field from **ACE3P** to **IMPACT-T** for particle tracking. Fig. 5 shows the integrated simulation for calculating the beam emittance as a function of the longitudinal position in the FACET-II injector, which includes an rf gun, an S-band accelerating structure and a solenoid between them. **Omega3P** is used to solve for the electromagnetic fields of the accelerating modes of the rf gun and the accelerating structure to produce the respective 3D field maps, which are then read into **IMPACT-T** for particle tracking of a low energy beam using the field maps for the full length of the injector. This integrated simulation at the system scale has been performed using the NERSC supercomputers.

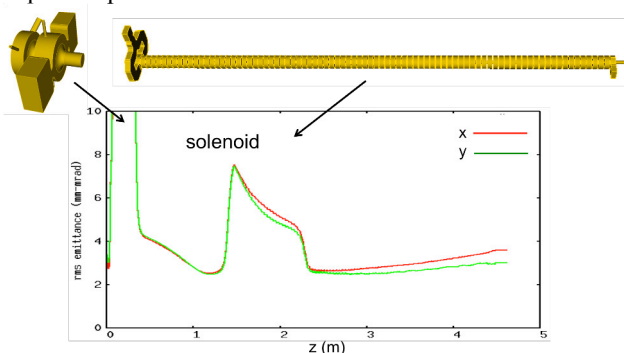


Figure 5: Beam emittances in the transverse directions for the FACET-II injector.

INTERFACE OF ACE3P TO RADIATION CALCULATION

Accelerator cavities operating at high gradients are subject to damage from high-energy electrons hitting the surface of the cavity wall. These electrons are believed to originate from certain locations of the cavity surface due to field emission, and then accelerated under the rf field of the cavity before impacting the cavity wall. Then, they will interact with the cavity wall made of certain materials and produce electromagnetic radiation that can affect the performance of the accelerator. For instance, during the commissioning of cryomodules at Jefferson Lab, strong radiation dosages along the cryomodules were observed during the processing period, regardless of the presence of the beam [8].

ACE3P provides simulation modules that model the 3D electromagnetic fields in an accelerator cavity, generate the initial field emission electrons, and track the electrons in the vacuum region of the cavity. When the electrons hit the cavity wall, their phase space information can be transferred to a particle-material interaction code such as Geant4 [9] or Fluka [10] for radiation calculation. Fig. 6 shows the calculation of the radiation dose for the LCLS-II cryomodule. **Track3P** is used to simulate dark current in a LCLS-II cavity, and an interface has been developed to transfer particle data on the cavity surface

from **Track3P** to Fluka to calculate radiation produced by the interaction of electrons with the wall materials [11].

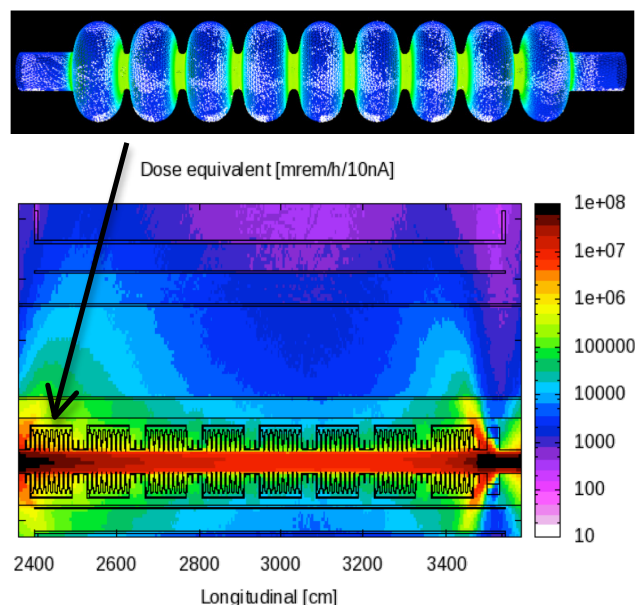


Figure 6: Interface of ACE3P dark current calculation (Top) to Fluka radiation calculation (Bottom).

ACKNOWLEDGEMENTS

We would like to thank Mario Santana for the Fluka radiation calculation. This research used resources of the National Energy Research Scientific Computing Center, which is supported by the Office of Science of the U.S. Department of Energy under Contract No. DE-AC02-05CH11231.

REFERENCES

- [1] https://portal.slac.stanford.edu/sites/ard_public/acd/Pages/Default.aspx
- [2] K. Ko et al., "Advances in Parallel Computing Codes for Accelerator Science and Development," Proc. LINAC2010, Tsukuba, Japan, 2010.
- [3] O. Kononenko, L. Ge, K. Ko, Z. Li, C.-K. Ng, L. Xiao, "A Massively Parallel Finite-Element Eigenvalue Solver for Modal Analysis in Structural Mechanics," Technical Report SLAC-PUB-15976, SLAC, 2014.
- [4] L. Xiao et al., "TTF Power Coupler Thermal Analysis for LCLS-II CW Application," these proceedings, IPAC'15, Richmond, USA(2015).
- [5] A. Hocker, "LCLS-II Coupler Test Results," FNAL presentation, 2014.
- [6] Z. Li et al., "Multi-Physics Analysis of CW Superconducting Cavity for the LCLS-II Using ACE3P," Proc. IPAC14, Dresden, Germany, 2014.
- [7] <http://amac.lbl.gov/~jiqiang/IMPACT-T/index.html>
- [8] F. Marhauser et al., "Field Emission and Consequences as Observed and Simulated for CEBAF Upgrade Cryomodules," Proc. of SRF 2013, Paris, Sep 23-27, 2013.
- [9] <http://geant4.cern.ch/>
- [10] https://www.fluka.org/fluka.php?id=secured_intro
- [11] C. Adolphsen, "High Power RF Status," LCLS-II DOE Review, April 7-9, 2015, SLAC.